Acta of Bioengineering and Biomechanics
Vol. 26, No. 1, 2024

Original paper
DOI: 10.37190/ABB-02351-2023-03

Properties of biodegradable polymer coatings with hydroxyapatite on a titanium alloy substrate

KAROLINA GOLDSZTAJN[1]*, MARCIN GODZIERZ[2], ANNA HERCOG[2], MARIUSZ WŁADOWSKI[3], JOANNA JAWORSKA[2], KATARZYNA JELONEK[2], ANNA WOŹNIAK[4], WOJCIECH KAJZER[1], ADA ORŁOWSKA[1], JANUSZ SZEWCZENKO[1]

[1] Silesian University of Technology, Faculty of Biomedical Engineering, Department of Biomaterials and Medical Device Engineering, Zabrze, Poland.
[2] Polish Academy of Science, Centre of Polymer and Carbon Materials, Zabrze, Poland.
[3] Optotom, Warszawa, Poland.
[4] Silesian University of Technology, Faculty of Mechanical Engineering, Department of Materials Engineering and Biomaterials, Gliwice, Poland.

Purpose: Titanium alloys are among the most widely used materials in medicine, especially in orthopedics. However, their use requires the application of an appropriate surface modification method to improve their properties. Such methods include anodic oxidation and the application of polymer coatings, which limit the release of alloying element ions. In addition, biodegradable polymer coatings can serve as a carrier for drugs and other substances. The paper presents the results of research on the physical properties of biodegradable polymer coatings containing na-noparticle hydroxyapatite on a titanium alloy substrate. *Methods*: A PLGA coating was used in the tests. The coatings on the substrate of the anodized Ti6Al7Nb alloy were applied by ultrasonic spray coating. The tests were carried out for coatings with various hydroxyapatite content (5, 10, 15, 20%) and thickness resulting from the number of layers applied (5, 10, 15 layers). The scope of the research included microscopic observations using scanning electron microscopy, topography tests with optical profilometry, structural studies using X-ray diffraction, as well as wettability and adhesion tests. *Results*: The results shows that with the use of ultrasonic spray coating system is possible to obtain the continuous coatings containing hydroxyapaptite. *Conclusions*: The properties of the coating can be controlled by changing the percentage of hydroxyapatite and the number of layers of which the coating is composed.

Key words: *titanium alloys, hydroxyapatite, adhesion of coatings, biodegradable polymer coatings, physical properties of coatings*

1. Introduction

More and more osteosynthesis procedures and surgical interventions are being performed due to the increase in fractures and their long-term effects [4]. Such a trend calls for continued development in the field of biomaterials and the search for better and better solutions. For this reason, it is observed that the basic direction is the study of surface modifications and their impact on the properties of materials, and consequently the improvement of the quality of the proposed final product solutions [23].

Methods that make it possible to modify the surface of titanium alloys include mechanical, chemical and physical processing. The most important properties that must be met by the type of surface modification used are efficiency, repeatability and cost-effectiveness. The surface layer produced must be characterized by deformability, Young's modulus value close to that of the substrate, hardness and brittleness corresponding to the substrate. In addition, the modification methods used must not cause phase and structural transformations [21].

One of the most commonly used biomaterials are titanium alloys. This is due to their good biocompati-

* Corresponding author: Karolina Goldsztajn, Silesian University of Technology, Faculty of Biomedical Engineering, Department of Biomaterials and Medical Device Engineering, Zabrze, Poland. E-mail: karolina.goldsztajn@polsl.pl
Received: November 28th, 2023
Accepted for publication: May 16th, 2024

bility in the environment of body fluids and tissues, low density, Young's modulus closest to that of bone the most among metallic materials and high corrosion resistance [16]. Titanium 6-aluminum 4-vanadium alloy and titanium 6-aluminum 7-nobium alloy are one of the most popular titanium alloys. They were thought to be of low reactivity and biologically inert. However, it has now been proven after many years of research that they are not completely biologically inert, as they can cause adverse reactions and allergies. This is due to the release of ions of alloying elements such as aluminum, vanadium or niobium [13].

Improving biocompatibility by reducing the release of ions from the surface of implants can be achieved through various surface modification methods. One of these is the anodic oxidation process, during which passive layers are produced on the surface of titanium alloy under the application of voltage in an electrolyte bath [9]. The morphology of the passive layers obtained by anodic oxidation depends on the applied voltage. At voltages above 150 V, porous layers are achieved. At a voltage below 40 V, in a bath with a low concentration of fluoride ions, it is possible to produce nanotube layers. To ensure osteoconductive values, anodic oxidation is carried out at medium voltages. As a result of the process carried out under such conditions, the resulting passive layer is dominated by TiO_2 oxide, with a small proportion of alloying element oxides. Depending on the voltage applied, we get different surface color effects. So far, two theories have been developed on this subject. The first is that the color obtained depends on the stoichiometric proportion of the individual oxides in the passive layer. The second is that it results from the differential interference of waves in different layer thicknesses. It has now been proven that the main cause of color creation is the interference of waves in the transitional oxide layer of titanium. For this reason, the different colors obtained during anodic oxidation depend only on the thickness of the resulting anodic layer. On the other hand, the thickness of the obtained layer depends on the value of the applied voltage, with its increase, an increase in the thickness of the passive layer is observed. The passive layers obtained by this process are up to several hundred nanometers thick and inherit the surface topography resulting from the previously implemented surface modification methods. Through anodic oxidation, we achieve improved resistance to pitting corrosion. In addition, this process limits the penetration of ions from the implant surface into the tissue environment but does not eliminate it entirely [8], [17].

Another possibility to reduce the release of degradation products into the body environment is the application of polymer coatings [19]. Moreover, in addition to improving biocompatibility, biodegradable polymer coatings may be a biodegradable drug delivery system, providing a matrix for active ingredients [7], [10]. As the polymer coating degrades, the locally released drug can enhance the bone healing process and reduce the need for systemic medication. Due to its low systemic toxicity, one of the most popular biodegradable polymers used for drug carriers is poly(lactic acid) (PLA) and polyglycolide (PGA) copolymer – poly(lactic-co--glycolic acid) (PLGA). Its minimal toxicity is a result of the fact that in the process of hydrolysis, it breaks down into PLA and PGA monomers, which, in turn, are easily metabolized by the body in the Krebs cycle. Its degradation time can take from several months, even up to several years, and can be controlled by changes in molecular weight and copolymer ratio [15]. Polymer coatings can be further enriched with substances that promote osteointegration such as bone morphogenetic protein (rhBMP-2) or fibroblast growth factors (bFGF)], which, when superimposed with PLGA by electrospraying, form homogeneous coatings on the titanium substrate, inheriting its surface roughness [5]. PLGA nanocomposites have been proven to improve biocompatibility while enabling targeted delivery of drugs or other nanosubstances. In addition, the use of a metal substrate ensures adequate mechanical properties throughout the treatment, while, at the same time, providing the benefits of a biodegradable polymer coating [11].

Hydroxyapatite (HAp) is the main component of the inorganic substance from which bones and tooth enamel are built. Bone apatite accounts for about 60–70% of the mass of bones, and its content varies depending on the type of bone, as well as age and the manner of recovery. Moreover, in the body, it is subject to continuous processes of dissolution, recrystallization and hydrolysis [24]. Because of that, synthetic hydroxyapatite (a ceramic material), is widely used in medicine. Of course, this is due to its osteoconductive properties and its similarity to the natural inorganic component of bone. However, it possesses a low resorption rate *in vivo* and is brittle. To solve these problems, HAp can be used in the form of a coating on the metal surface. Such a solution allows to preserve the mechanical properties of the metal, while improving the process of bone fusion and significantly improving the resistance of the metal implant to corrosion in body tissue environment [12]. Such hydroxyapatite coatings can be applied to a metal surface by a variety of physical and chemical methods. Some of the most commonly used methods of applying HAp to a surface include electrochemical deposition, sol-gel method or plasma spraying [6], [17], [18]. Another solution is to combine hydroxyapatite with a polymer, such as biodegradable PLGA [2], [6].

Today, biodegradable polymer-bioceramic composites are often used. The addition of biodegradable polymers such as poly(glycolic acid), poly(lactic acid) and poly(D,L-lactic-co-glycolic acid) (PLGA) to calcium phosphate ceramics would allow for better manipulation and control of both macro- and microstructure in shaping composites to fit bone defects. In addition, biodegradable polymers could be used as binders for HA or other calcium phosphate-based ceramics to reduce their brittleness [10].

A promising idea seems to be the application of biodegradable polymer coatings enriched with hydroxyapatite on the titanium alloy substrate. During the degradation of the polymer, HAp is released to improve the bone healing process. In addition, the use of polymer in the form of a coating does not lead to a loss of mechanical properties of the implant with the time of the polymer degradation process. Also, such a solution leads to improved biocompatibility by reducing the penetration of alloying element ions into the tissue environment as a result of the degradation process.

Nowadays, the dip-coating method is one of the most commonly used methods of applying polymer coatings. Recently, also the ultrasonic spraying method has become popular. This method involves spraying fine droplets onto the surface of the material and allows to obtaining continuous, homogeneous coatings, characterized by good adhesion to the substrate and properties that can be controlled by changing process parameters. In addition, the use of the ultrasonic method can produce thinner layers than the dip coating method, with evenly dispersed nanoparticles. This is due to the possibility of using a magnetic stirrer throughout the polymer coating application process [3].

The presented paper addresses innovations in the context of known polymer-ceramic composite coatings with HAp applied to titanium alloy substrate. The aim of the work was to determine the impact of various numbers of coating layers and amount of hydroxyapatite on the physical and chemical properties of the surface. To determine the physical and chemical properties of the obtained biodegradable polymer coatings containing hydroxyapatite, the following tests were carried out: surface observation, topography and wettability studies, structural investigation and adhesion of the coatings to the metal substrate.

2. Materials and methods

A Ti6Al7Nb alloy with chemical composition, structure, and mechanical properties complying with ISO 5832-11 recommendations was used as a substrate. The samples were taken from a rod with a diameter of 25 mm (Fig. 1). The surface of the substrate was modified by grinding, sandblasting and anodic oxidation. Abrasive papers of 120, 300 and 500 grade, respectively, were used for the grinding. Sandblasting was carried out for t = 2 min with SiO_2 balls of diameter from 70 to 110 μm. Anodization was performed with the use of a bath based on phosphorous and sulphuric acid (Titan Color, Poligrat GmbH) at the voltage of 97 V; t = 2 min. Before the coating process, the samples were purified in 99% isopropanol.

Polymer coatings based on poly(D,L-lactide-glycolide) PLGA(85/15) with hydroxyapatite (HAp) (Merck, crystallite size up to 200 nm) were chosen for the coating materials. PLGA was synthesized in bulk by the ring opening polymerization of glycolide (Purac) and D,L-lactide (Purac) at 130 °C for 24 hours and next, at 120 °C for 48 hours at argon atmosphere using Zirconium (IV) acetylacetonate (Zr(acac)4) (Merck) as a non-toxic initiator.

The metallic substrate was coated with the polymer by the ultrasonic spray coating method. The solution of 1% PLGA in dichloromethane was enriched with 5, 10, 15 or 20% HAp. The coatings were applied by ExactaCoat (Sono-Tek) with AccuMist™ Ultrasonic Spray Shaping with the following parameters of the process: ultrasound frequency 60 kHz, ultrasound power of 1.5 W, solution's flow rate of 1 cm^3/min, speed of nozzle motion of 10 mm/s, the distance between nozzle and substrate surface of 70 mm and air curtain pressure of 2 Pa. The coatings consisted of 5, 10 or 15 layers. The coated samples were airdried for 3 days at 25 °C.

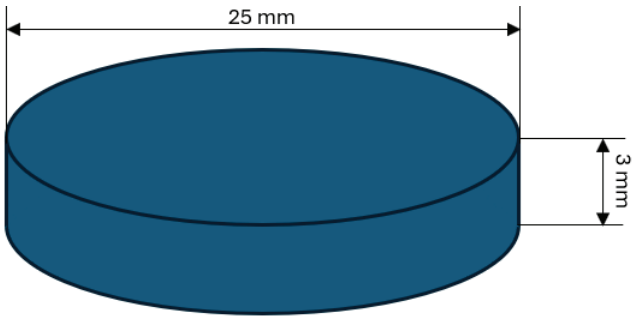

Fig. 1. Diagram of the tested samples

2.1. Surface observation

The morphology of the samples was analyzed using a scanning electron microscope (SEM) Quanta 250 FEG, Thermo Fisher Scientific, operating under low

vacuum conditions (80 Pa) and the acceleration voltage of 10 kV from secondary electrons collected by a Large Field Detector. The observations were carried out using backscattered electrons collected by the low-voltage high-contrast detector (vCD) which gives an atomic-number (Z) contrast. For each sample, 5 surface images were taken in different areas.

2.2. Topography studies

The surface topography studies were carried out with a Sensofar Sneox optical profilometer. A combination of two scanning techniques was applied: confocal and focal differentiation for each measured frame (Confocal Fusion). Light with a wavelength of 530 nm and a 20× magnification lens were used. The tests were carried out on the surface of 3200 × 2600 μm. Five samples from each variant were used for testing, and 3 measurements were taken for each. Ra (profile roughness avarage – the arithmetic mean of the absolute values of the surface height deviations from the mean line) and Sa (areal average roughness – the average height of all measured points in the areal measurement) parameters, determined in accordance with ISO 21920 and ISO 25178, respectively, were selected for analysis.

2.3. Wettability tests

The wettability of the surface was determined based on the contact angle. Contact angle measurements were performed with Biolin Scientific Attension Theta Flex optical tensiometer and analyzed using OneAttension software. The tests were carried out using distilled water with a droplet size of 1.5 mm^3. The measurement started 15 s after the drop deposition and lasted 60 s with a sampling rate of 1 Hz. Five measurements were taken on each sample. The population of samples of each variant used in the study was three.

2.4. X-Ray diffraction studies

X-Ray diffraction (XRD) studies were performed using the D8 Advance diffractometer (Bruker, Karlsruhe, Germany) with Cu-Kα cathode (λ = 1.54 Å) operating at 40 kV voltage and 40 mA current. The scan rate was 0.60°/min with scanning step 0.02° in a range of 5° to 90° 2θ. Identification of fitted phases was performed using DIFFRAC.EVA program with the use of Crystallography Open Database (COD) and International Centre for Diffraction Data database (ICDD PDF#2), while exact lattice parameters and atomic coordinates of fitted phase were calculated using Rietveld refinement in TOPAS 6 program, based on Williamson–Hall theory. The pseudo-Voigt function was used in the description of diffraction line profiles at the Rietveld refinement. The R_{wp} (weighted-pattern factor), R_{exp} (expected R factor) and GOF (goodness-of-fit) parameters were used as numerical criteria of the quality of the fit of calculated to experimental diffraction data. XRD tests were carried out both for the hydroxyapatite powder used in the tests and for the applied polymer coatings.

2.5. Adhesion study

The tests on the adhesion of the biodegradable polymer coatings to the substrate were performed by the scratch test method, using the open platform with MicroCombi Tester by CSM (Anton Paar). A diamond Rockwell cone intender was used for the study. The loading force was increasing from 0.03 to 30 N. The force load rate was 10 N/min, the table travel speed was 1 mm/min, and the scratch length was 3 mm. Due to the difficulty in estimating the critical force F_n, using microscopic observation, a comparison of the obtained friction force as a function of the scratch length for the non-coated and coated samples was proposed. The first intersection point of the curves was treated as the force causing the delamination of the coating [20]. Five samples from each variant were used for the tests. Three measurements were taken on each sample.

2.6. Statistical analysis

All results reported in this paper are presented as means with standard deviation. To determine the significance of differences for $p < 0.05$, one-way analysis of variance (ANOVA) was used in the obtained results.

3. Results

3.1. Surface observation

The surfaces of all polymer coatings regardless of the amount of HAp and the number of layers applied were characterized by continuity (Fig. 2). Hydroxyapatite (light points on the SEM images) is characterized by a homogeneous dispersion over the whole surface of the sample. Clusters of HAp can be observed in the

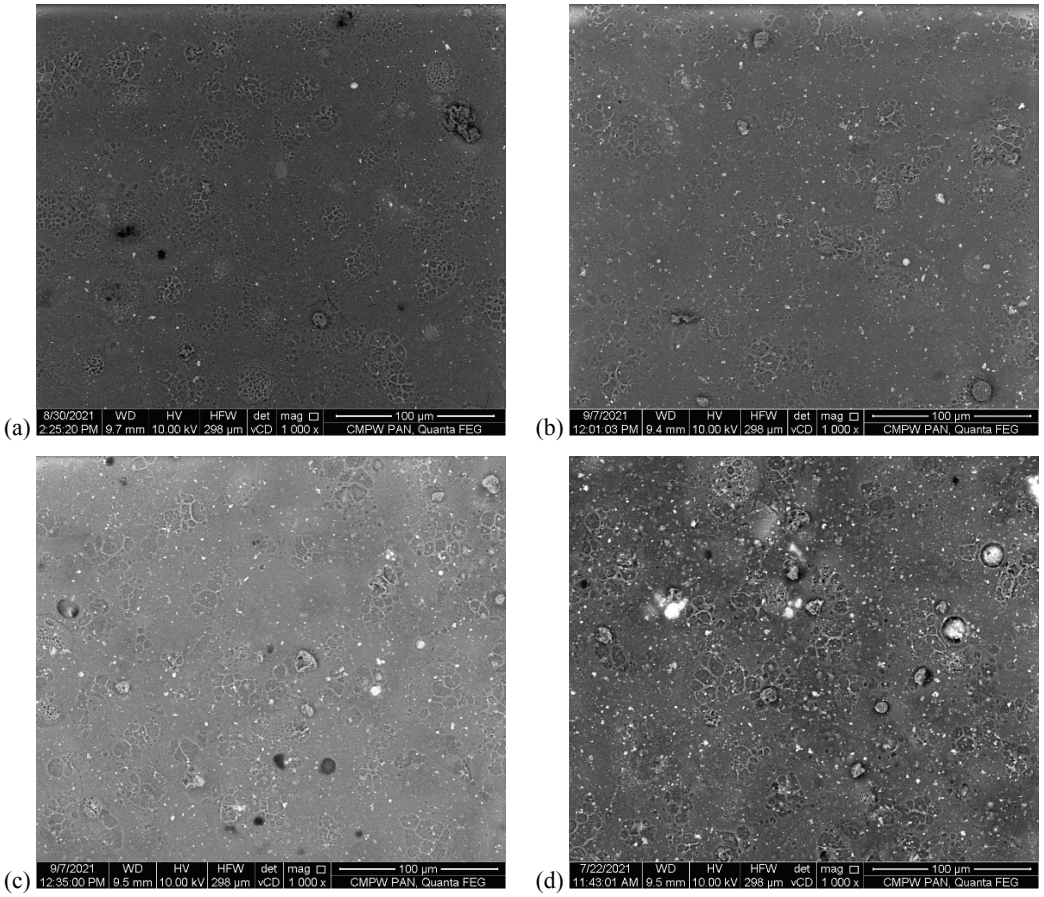

Fig. 2. Surface topography of 15-layer polymer coatings containing: (a) 5%, (b) 10%, (c) 15%, (d) 20% of HAp (SEM)

coating, the number and size of which increased with an increase in the concentration of hydroxyapatite and the number of layers, indicating aggregation of HAp particles resulting from an increase in the amount of HAp in the coating (marked by arrows). In addition, characteristic effects from the solvent evaporation process can be observed on the surface, marked with circles in Fig. 2.

3.2. Topography studies

Based on the obtained roughness results, an increase in the value of the Ra parameter was observed with an increase in the number of layers (Table 1). The percentage of HAp content had an ambiguous effect on the *Ra* values. However, in the case of the Sa parameter, no unequivocal effect of the influence of the number of applied layers and HAp concentration was observed (Table 2). The coatings consisting of 10 layers were characterized by the highest Sa values. Examples of topography images are shown in Fig. 3. In addition, statistical analysis shows that both the number of layers and the concentration of hydroxyapatite have no statistically significant effect on the value of the Ra parameter ($p > 0.5$). However, in the case of the Sa parameter, the effect of the number of layers and HAp concentration was noted to be statistically significant (p-value in the range of $0.1 \cdot 10^{-3}$–$0.3 \cdot 10^{-3}$), except for a coating consisting of 15 layers, for which the change in concentration is not statistically significant.

Table 1. Results of Ra parameter

Ra [µm]				
HAp % / Layers	5%	10%	15%	20%
5 layers	0.87 (45)	0.86 (24)	0.76 (48)	0.82 (59)
10 layers	1.01 (31)	1.05 (58)	0.99 (25)	0.83 (36)
15 layers	1.16 (39)	1.28 (46)	1.16 (19)	1.03 (43)

Table 2. Results of Sa parameter

Sa [µm]				
HAp % / Layers	5%	10%	15%	20%
5 layers	2.25 (54)	1.71 (19)	1.00 (37)	1.08 (48)
10 layers	3.61 (40)	3.98 (28)	4.61 (51)	3.24 (25)
15 layers	1.39 (26)	1.35 (57)	1.38 (43)	1.17 (39)

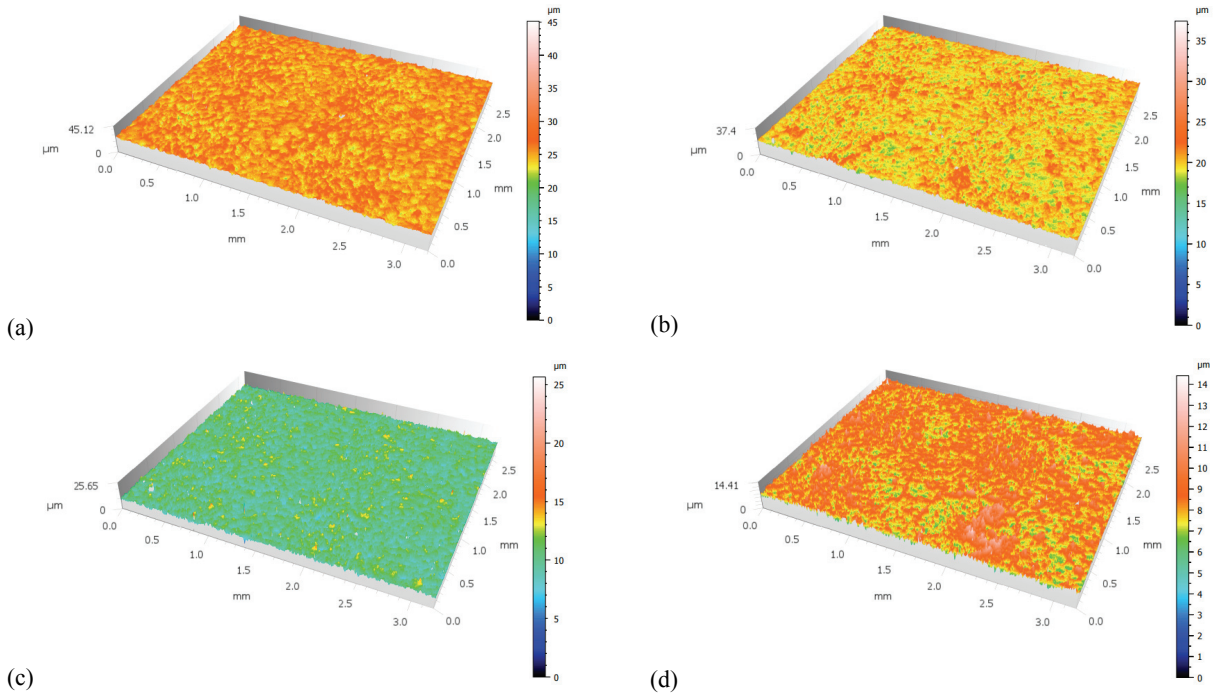

Fig. 3. Topography of 5-layer PLGA coating containing: (a) 5%, (b) 10%, (c) 15%, (d) 20% of HAp

3.3. Wettability tests

The analyzed surfaces of polymer coatings were characterized by a hydrophilic surface with a contact angle in the range of 81.4–87.6°. Neither the hydroxyapatite content nor the number of applied coatings had any effect on the wettability of the surface (Table 3). Statistical analysis did not indicate a statistically significant effect on the contact angle value of the number of layers the coating consisted of and the amount of HAp ($p > 0.05$).

Table 3. Wettability of PLGA polymer coatings surface

Contact angle Θ [°]				
HAp % / Layers	5%	10%	15%	20%
5 layers	86.4 (32)	86.3 (24)	85.4 (20)	85.5 (23)
10 layers	81.4 (19)	85.7 (56)	83.7 (45)	87.6 (44)
15 layers	84.1 (54)	83.5 (43)	83.8 (33)	85.4 (52)

3.4. XRD studies

A typical XRD pattern of hydroxyapatite powder is presented in Fig. 4. Rietveld refinement shows that the main phase in examined powder is $Ca_{10}(PO_4)_6(OH)_2$, while minor amount of $Ca_4(PO_4)_2O$ and traces of $Ca(OH)_2$ and $Ca_3(PO_4)_2$ were detected. The crystallite size of the main phase is in good agreement with producer data (180 nm vs. 200 nm), while other phases show much lower crystallite size – up to 50 nm (Table 4). Lattice strain was only detected for the HAp phase with low value. Performed Rietveld refinement studies show lattice parameters of $Ca_{10}(PO_4)_6(OH)_2$, $Ca(OH)_2$ and $Ca_4(PO_4)_2O$ with good agreement with model data.

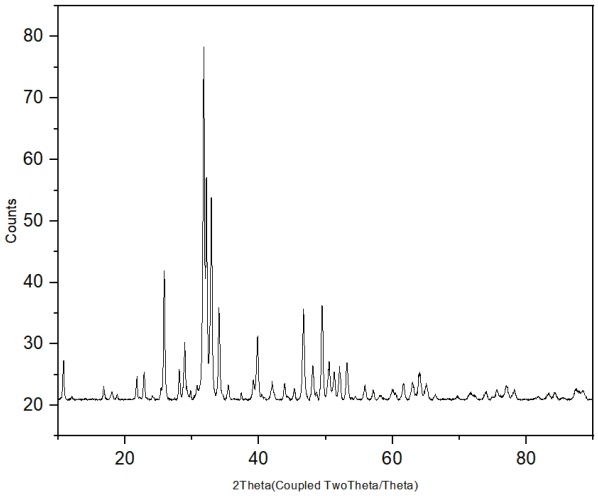

Fig. 4. XRD pattern of hydroxyapatite powder

In Figures 5–8, XRD patterns typically acquired for PLGA/HAp coatings on Ti6Al7Nb substrate with various amounts of HAp and variable layer thickness are shown, while in Table 5, structural parameters of crys-

Table 4. Crystallographic parameters calculated for identified phases of HAp powder.
Values in brackets represent the variation coefficient, not the standard deviation

Phase name	Model parameters [Å]	Calculated parameters [Å]	Crystallite size [nm]	Lattice strain [%]	Weight amount [%]
$Ca_{10}(PO_4)_6(OH)_2$	$a = b = 9.424$, $c = 6.879$	$a = b = 9.428$, $c = 6.888$	180 (30)	0.289 (13)	96.81 (5)
$Ca(OH)_2$	$a = b = 3.589$, $c = 4.911$	$a = b = 3.583$, $c = 4.919$	33 (13)	0	0.83 (4)
$Ca_4(PO_4)_2O$	$a = 7.023$, $b = 11.986$, $c = 9.473$, $\beta = 90.9°$	$a = 7.355$, $b = 11.996$, $c = 9.477$, $\beta = 86.3°$	48 11)	0	2.21 (5)
$Ca_3(PO_4)_2$	$a = b = 5.249$, $c = 18.674$	$a = b = 5.207$, $c = 19.169$	7 (1)	0	0.15 (2)

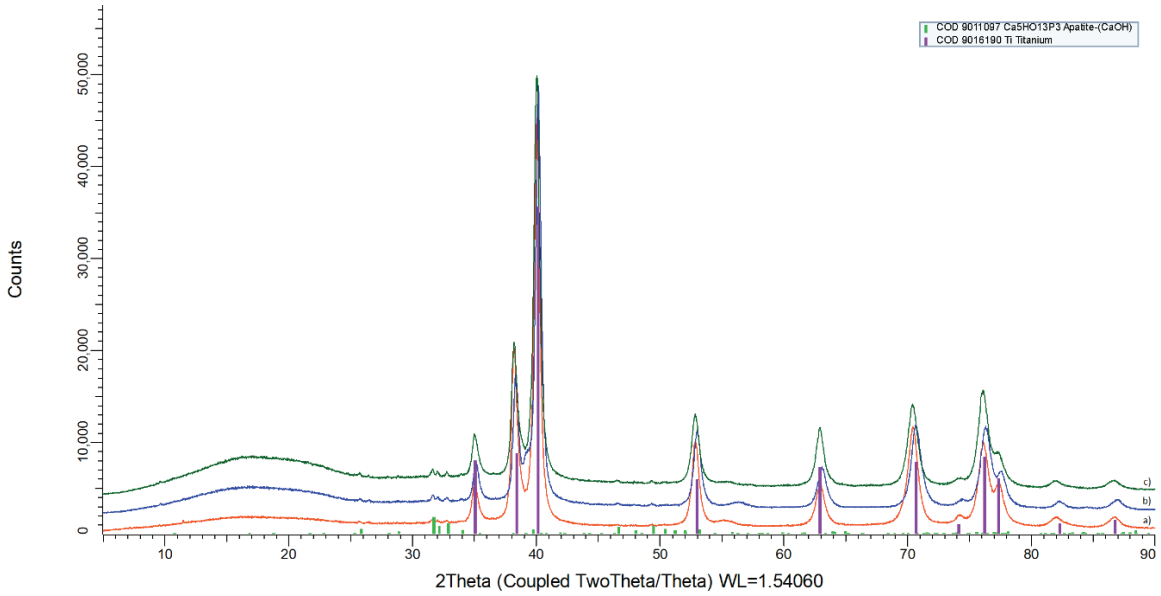

Fig. 5. XRD patterns of PLGA/HAp coating with 5 wt.% of HAp and various layers: (a) 5 layers, (b) 10 layers and (c) 15 layers; patterns were offset along *Y*-axis for better comparison

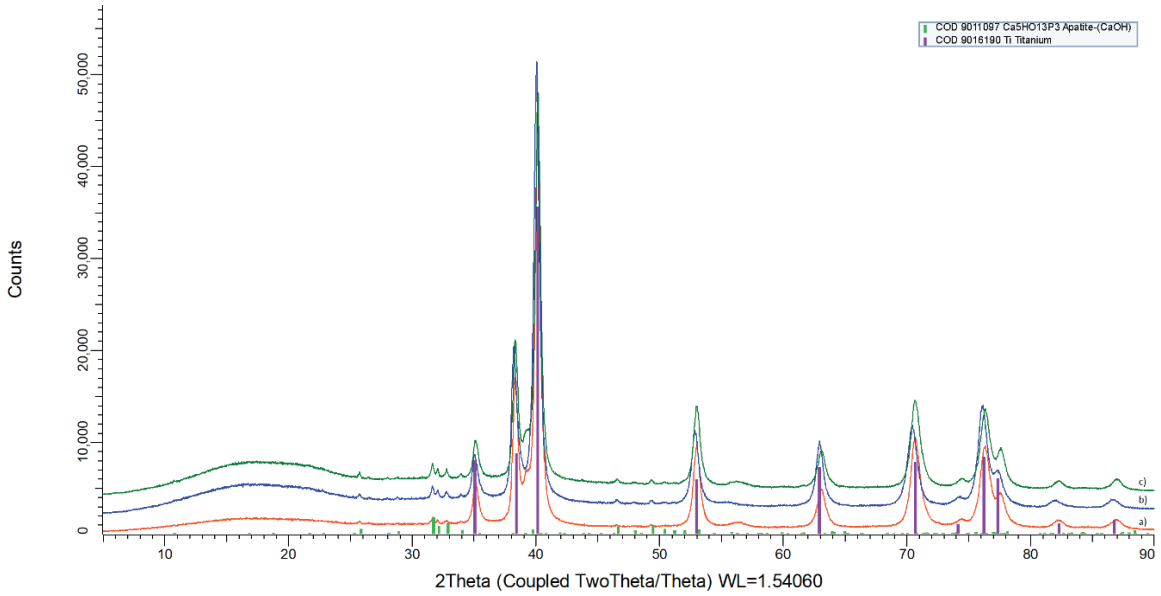

Fig. 6. XRD patterns of PLGA/HAp coating with 10 wt.% of HAp and various layers: a) 5 layers, b) 10 layers and c) 15 layers; patterns were offset along *Y*-axis for better comparison

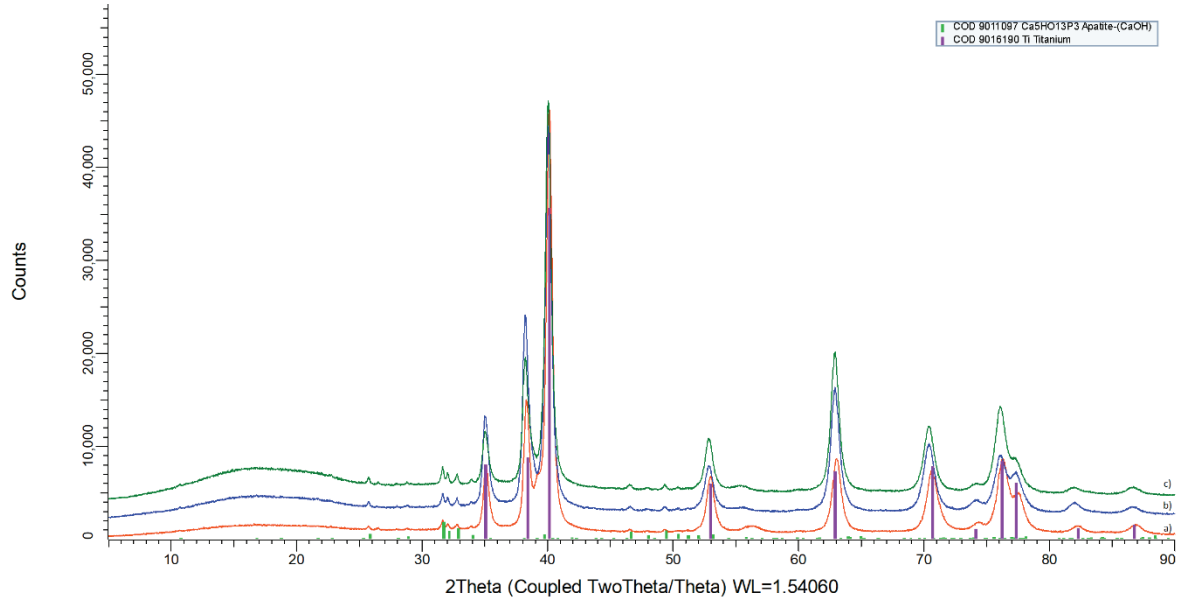

Fig. 7. XRD patterns of PLGA/HAp coating with 15 wt.% of HAp and various layers: a) 5 layers, b) 10 layers and c) 15 layers; patterns were offset along the *Y*-axis for better comparison

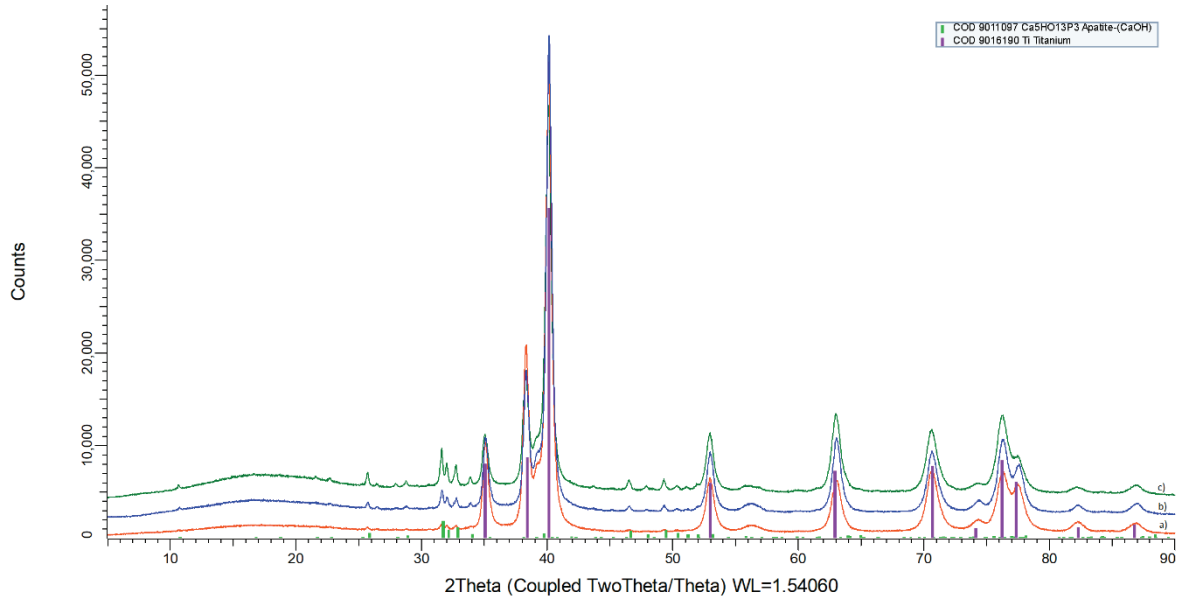

Fig. 8. XRD patterns of PLGA/HAp coating with 20 wt.% of HAp and various layers: a) 5 layers, b) 10 layers and c) 15 layers; patterns were offset along *Y*-axis for better comparison

talline phases detected in samples are listed. All detected peaks belong to α-/β-titanium and hydroxyapatite phases, indicating a lack of PLGA crystallization. Determined lattice parameters of both, α- and β-titanium, independently of layer thickness and HAp amount, are stable with some negligible variations. As can be seen, with an increase in layer thickness, the amount of amorphous PLGA phase increases, visible as a broad halo in 8–25° 2θ in Figs. 1–4. Simultaneously, the increase of HAp peaks occurs and its weight amount increases (Table 1). On the other hand, an increment of HAp amount in coating leads to a decrease of amorphous phase content.

Structural studies using Rietveld refinement (Table 1) show a decrease in lattice strain of hydroxyapatite with an increase in layer thickness. The highest lattice strain was detected for coatings with 20 wt.% of HAp nanoparticles, most likely as a result of its high amount, which allows for stronger interactions with each other during sonication.

Table 5. Selected structural parameters of crystalline phases determined using Rietveld refinement; values in brackets represent variation coefficient, not standard deviation

Sample	Phase (*space group*)	Lattice parameters, ICDD [Å]	Lattice parameters, calculated [Å]	Crystallite size [nm]	Lattice strain [%]	Weight amount [%]
1	**2**	**3**	**4**	**5**	**6**	**7**
5%, 5 layers	$Ca_{10}(PO_4)_6(OH)_2$ ($P6_3/m$)	$a = b = 9.424$, $c = 6.879$	$a = b = 9.460$, $c = 6.910$	200 (16)	1.19 (7)	2.0 (8)
	α-Ti ($P6_3/mmc$)	$a = b = 2.95$, $c = 4.68$	$a = b = 2.952$, $c = 4.699$	30 (11)	0.90 (4)	87.5 (8)
	β-Ti ($Im\text{-}3m$)	$a = 3.30$	$a = 2.98$	3 (6)	0	10.5 (7)
5%, 10 layers	$Ca_{10}(PO_4)_6(OH)_2$ ($P6_3/m$)	$a = b = 9.424$, $c = 6.879$	$a = b = 9.452$, $c = 6.900$	200 (12)	1.09 (5)	2.2 (9)
	α-Ti ($P6_3/mmc$)	$a = b = 2.95$, $c = 4.68$	$a = b = 2.945$, $c = 4.683$	30 (12)	0.87 (4)	87.3 (9)
	β-Ti ($Im\text{-}3m$)	$a = 3.30$	$a = 2.98$	3 (6)	0	10.5 (7)
5%, 15 layers	$Ca_{10}(PO_4)_6(OH)_2$ ($P6_3/m$)	$a = b = 9.424$, $c = 6.879$	$a = b = 9.449$, $c = 6.910$	200 (11)	1.01 (5)	2.9 (9)
	α-Ti ($P6_3/mmc$)	$a = b = 2.95$, $c = 4.68$	$a = b = 2.954$, $c = 4.699$	30 (12)	0.95 (4)	86.6 (9)
	β-Ti ($Im\text{-}3m$)	$a = 3.30$	$a = 2.98$	3 (6)	0	10.5 (7)
10%, 5 layers	$Ca_{10}(PO_4)_6(OH)_2$ ($P6_3/m$)	$a = b = 9.424$, $c = 6.879$	$a = b = 9.453$, $c = 6.896$	200 (19)	1.20 (4)	3.0 (7)
	α-Ti ($P6_3/mmc$)	$a = b = 2.95$, $c = 4.68$	$a = b = 2.946$, $c = 4.685$	30 (11)	0.86 (3)	86.5 (7)
	β-Ti ($Im\text{-}3m$)	$a = 3.30$	$a = 2.98$	3 (6)	0	10.5 (7)
10%, 10 layers	$Ca_{10}(PO_4)_6(OH)_2$ ($P6_3/m$)	$a = b = 9.424$, $c = 6.879$	$a = b = 9.445$, $c = 6.903$	200 (16)	1.12 (3)	3.5 (8)
	α-Ti ($P6_3/mmc$)	$a = b = 2.95$, $c = 4.68$	$a = b = 2.952$, $c = 4.699$	30 (11)	0.85 (3)	85.5 (8)
	β-Ti ($Im\text{-}3m$)	$a = 3.30$	$a = 2.98$	3 (6)	0	10.5 (7)
10%, 15 layers	$Ca_{10}(PO_4)_6(OH)_2$ ($P6_3/m$)	$a = b = 9.424$, $c = 6.879$	$a = b = 9.453$, $c = 6.903$	200 (16)	1.05 (3)	6.2 (10)
	α-Ti ($P6_3/mmc$)	$a = b = 2.95$, $c = 4.68$	$a = b = 2.947$, $c = 4.686$	30 (12)	0.76 (4)	83.3 (10)
	β-Ti ($Im\text{-}3m$)	$a = 3.30$	$a = 2.98$	3 (6)	0	10.5 (7)
15%, 5 layers	$Ca_{10}(PO_4)_6(OH)_2$ ($P6_3/m$)	$a = b = 9.424$, $c = 6.879$	$a = b = 9.450$, $c = 6.901$	200 (30)	1.23 (2)	4.0 (5)
	α-Ti ($P6_3/mmc$)	$a = b = 2.95$, $c = 4.68$	$a = b = 2.948$, $c = 4.686$	30 (8)	0.92 (2)	85.5 (5)
	β-Ti ($Im\text{-}3m$)	$a = 3.30$	$a = 2.98$	3 (6)	0	10.5 (7)
15%, 10 layers	$Ca_{10}(PO_4)_6(OH)_2$ ($P6_3/m$)	$a = b = 9.424$, $c = 6.879$	$a = b = 9.448$, $c = 6.902$	200 (30)	1.16 (2)	4.6 (6)
	α-Ti ($P6_3/mmc$)	$a = b = 2.95$, $c = 4.68$	$a = b = 2.953$, $c = 4.699$	30 (9)	0.98 (3)	84.9 (6)
	β-Ti ($Im\text{-}3m$)	$a = 3.30$	$a = 2.98$	3 (6)	0	10.5 (7)
15%, 15 layers	$Ca_{10}(PO_4)_6(OH)_2$ ($P6_3/m$)	$a = b = 9.424$, $c = 6.879$	$a = b = 9.457$, $c = 6.909$	200 (30)	1.11 (2)	7.3 (8)
	α-Ti ($P6_3/mmc$)	$a = b = 2.95$, $c = 4.68$	$a = b = 2.955$, $c = 4.702$	30 (12)	0.94 (3)	82.2 (8)
	β-Ti ($Im\text{-}3m$)	$a = 3.30$	$a = 2.98$	3 (6)	0	10.5 (7)

1	2	3	4	5	6	7
20%, 5 layers	$Ca_{10}(PO_4)_6(OH)_2$ ($P6_3/m$)	$a = b = 9.424$, $c = 6.879$	$a = b = 9.452$, $c = 6.898$	200 (16)	1.27 (3)	4.9 (5)
	α-Ti ($P6_3/mmc$)	$a = b = 2.95$, $c = 4.68$	$a = b = 2.946$, $c = 4.684$	30 (6)	0.93 (19)	84.6 (5)
	β-Ti ($Im\text{-}3m$)	$a = 3.30$	$a = 2.98$	3 (6)	0	10.5 (7)
20%, 10 layers	$Ca_{10}(PO_4)_6(OH)_2$ ($P6_3/m$)	$a = b = 9.424$, $c = 6.879$	$a = b = 9.45$, $c = 6.90$	180 (19)	1.21 (13)	7.2 (6)
	α-Ti ($P6_3/mmc$)	$a = b = 2.95$, $c = 4.68$	$a = b = 2.946$, $c = 4.684$	30 (7)	0.77 (2)	82.3 (6)
	β-Ti ($Im\text{-}3m$)	$a = 3.30$	$a = 2.98$	3 (6)	0	10.5 (7)
20%, 15 layers	$Ca_{10}(PO_4)_6(OH)_2$ ($P6_3/m$)	$a = b = 9.424$, $c = 6.879$	$a = b = 9.449$, $c = 6.90$	180 (12)	1.17 (8)	8.0 (6)
	α-Ti ($P6_3/mmc$)	$a = b = 2.95$, $c = 4.68$	$a = b = 2.948$, $c = 4.686$	30 (10)	0.91 (3)	81.5 (6)
	β-Ti ($Im\text{-}3m$)	$a = 3.30$	$a = 2.98$	3 (6)	0	10.5 (7)

3.5. Adhesion study

The obtained values of the critical force indicate that the worst adhesion of coatings to the substrate is exhibited by coatings consisting of 5 layers. With the increase in the number of layers, the adhesion of the coatings to the metal substrate increases. No unequivocal effect of the amount of HAp on the value of the critical force was observed. However, the highest F_n value showed a coating consisting of 15 layers with 20% HAp content. In addition, there is no statistically significant effect of hydroxyapatite concentration on F_n strength ($p > 0.05$). However, the analysis revealed a statistically significant effect of coating thickness (indicated by the number of layers) on the adhesion of the coating to the substrate ($p < 0.05$).

Table 6. Force causing delamination of coating

Critical force [N]				
HAp % / Layers	5%	10%	15%	20%
5 layers	0.93 (29)	0.87 (59)	1.03 (21)	0.96 (32)
10 layers	1.42 (42)	1.54 (19)	1.32 (53)	1.39 (43)
15 layers	2.03 (54)	2.54 (38)	2.34 (44)	2.63 (27)

4. Discussion

The results presented in this article show that it is possible to apply polymer coatings containing hydroxyapatite with fractions up to 200 nm by ultrasonic spraying. The obtained coatings were characterized by continuity and good dispersion of hydroxyapatite (Fig. 2). Polymer spheres and effects due to solvent evaporation were observed on the polymer surface, which are characteristic of the coating method used [3].

The addition of hydroxyapatite increases the roughness of the polymer coating. The Sa parameter for PLGA coatings without HAp produced by this method at the same parameters is 0.523 (59) μm, which is on average about 59% lower than the value of the Sa parameter of coatings containing HAp (statistically significant difference). A detailed analysis of the roughness measurements indicates that the value of the *Ra* parameter is affected by the number of layers applied, causing its value to increase with an increase in their number (Table 1). In contrast, the concentration of hydroxyapatite has an ambiguous effect on this value. Analysis of the Sa parameter did not show a clear effect of the number of layers or the amount of HAp on its value (Table 2).

The applied coatings regardless of the number of layers as well as the content of hydroxyapatite were characterized by hydrophilic properties (Table 3). The value of the contact angle was variable in the range 81.4(19)–87.6(44)°. Comparing the wettability of biodegradable PLGA polymer coatings obtained by ultrasonic spraying with coatings containing hydroxyapatite, it can be concluded that the addition of hydroxyapatite results in an increase in the contact angle. Coatings of pure PLGA were characterized by a contact angle of about 63.2(25)°, which resulting in an average increase in contact angle of about 34% for coatings consisting of 15 layers. Based on the ANOVA analysis, these differences were found to be statistically significant

($p < 0.05$). This effect may be due to two factors. First, the change in surface topography is caused by the presence of hydroxyapatite in the coating. Second, the presence of hydroxyapatite on the surface of the coating, for which the contact angle can vary over a wide range, depending on how the coatings are obtained or applied [1]. Polylactide PLA is a hydrophobic polymer. By the copolymerization with glycolide, the hydrophobic character of the polymer can be reduced – it is connected with the methylene groups – CH3 remaining in the LA units whose number is reduced after copolymerization. Varga et al. [22] measured the contact angles for different PLGA and their value decreased from 74.55° to 68.18° with decreasing amount of lactide part from 100% (PLA) to 65% (PLGA65). By the addition of the hydroxyapatite to the PLGA, the value of the water contact angle in our study increased, which is connected with the character of the HAp. In the PLGA + HAp system, the HAp particles are dispersed on the surface of the PLGA, as well as in the entire volume. For similar systems such as some polymeric carriers enriched with hydrophobic drugs, the surface concentration of the drug is also observed, which results in the burst effect of the drug [14].

A detailed analysis of the results of X-Ray diffraction studies of hydroxyapatite nanopowder showed the presence of the following phases $Ca_{10}(PO_4)_6(OH)_2$, $Ca_4(PO_4)_2O$, $Ca(OH)_2$ and $Ca_3(PO_4)_2$, the main one being $Ca_{10}(PO_4)_6(OH)_2$ with a percentage of 96.81% (Table 4). The size of the crystals of the main phase averaged 180 nm, which is in accordance with the producer's data. Other phases showed much lower crystallite size (up to 50 nm), which might suggest its formation on the surface of HA nanoparticles. In addition, detailed analysis showed lattice strain for the HAp phase, which suggests the presence of minor residual stress. Analysis of XRD spectra grounded for polymer coatings confirmed the presence of hydroxyapatite (Figs. 5–8). The decrease of lattice strain of hydroxyapatite with an increase in layer thickness is, most likely, a result of the impact of HAp particles during deposition on titanium substrate. Moreover, it was observed that as the HAp concentration increases, the intensity and separation of the peaks decreases. For coatings that contained 20% HAp, the highest lattice strain was detected. This suggests the partial formation of agglomerates of hydroxyapatite nanoparticles and is confirmed by observations made with scanning electron microscopy. The formation of agglomerates may be the result of a high HAp amount, which allows for stronger interactions with each other during sonication.

PLGA coatings containing hydroxyapatite applied by ultrasonic spraying showed good adhesion to the surface of anodically oxidized titanium alloy (Table 6). Adhesion of the coatings depended on the thickness of the coating. The greatest adhesion was characterized by coatings consisting of 15 layers. The hydroxyapatite content of the coating did not clearly affect its adhesion. Comparing the critical force of a pure PLGA coating consisting of 15 layers (1.43(28) N) with the results obtained for a coating containing hydroxyapatite, it can be clearly seen that regardless of the hydroxyapatite content in the coating, it improves the adhesion of the coating to the substrate. The increase in the value of the critical force causing delamination of the coating containing HAp with relation to the coating of neat PLGA is about 62%, and this difference is statistically significant ($p < 0.05$).

5. Conclusions

The use of an ultrasonic spray coating makes it possible to obtain coatings of biodegradable PLGA polymer containing hydroxyapatite on an anodically oxidized titanium alloy substrate. The physical properties of the produced coating can be modified by changing the hydroxyapatite content and the number of layers produced. In addition, it can be concluded that irrelevant to the number of coating layers applied, the use of hydroxyapatite increases the wetting angle (θ = 81.4(19) –87.6(44)°) and surface roughness (Sa = 1.00(37) 4.61(51) μm) relative to the biodegradable PLGA polymer coating applied by the same method, with the same parameters (θ = 63.2(25)°, Sa = 0.523(59) μm). Moreover, it was observed that biodegradable polymer coatings containing hydroxyapatite have higher adhesion to the metal substrate (for 15 layers F_n = 2.03(54)–2.63(27)N) than PLGA polymer coatings applied with the same parameters (1.43(28)N). The results of the study provide a basis for further research to determine the effect of in vitro conditions on the physical properties of the coatings, as well as polymer degradation and HAp release kinetics.

References

[1] ARONOV D., ROSEN R., RON E.Z., ROSENMAN G., *Tunable hydroxyapatite wettability: Effect on adhesion of biological molecules*, Process Biochemistry, 2006, Vol. 41, 2367–2372, DOI: https://doi.org/10.1016/j.procbio.2006.06.006

[2] ASTI A., GASTALDI G., DORATI R., SAINO E., CONTI B., VISAI L., BENAZZO F., *Stem Cells Grown in Osteogenic Medium on PLGA, PLGA/HA and Titanium Scaffolds for Surgical Applications*, Bioinorganic Chemistry and Application, 2010, DOI: 10.1155/2010/831031.

[3] BOSE S., KELLER S., ALSTROM T., BOISEN A., ALMDAL K., *Process optimalization of Ultrasonic Spray Coating of Polymer Films*, Langmuir, 2013, 29, 6911–6919, DOI: https://doi.org/10.1021/la4010246

[4] *GBD 2019 Fracture Collaborators: Global, regional, and national burden of bone fractures in 204 countries and territories, 1990–2019: a systematic analysis from the Global Burden of Disease Study 2019*, The Lancet, 2021, Vol. 2, 580–592.

[5] GHERASIM O., GRUMEZESCU A.M., GRUMEZESCU V., ANDRONESCU E., NEGUT I., BIRCA A.C., GALATEANU B., HUDITA A., *Bioactive Coatings Loaded with Osteogenic Protein for Metallic Implants*, Polymers (Basel), 2021, Vol. 13, DOI: 10.3390/polym13244303.

[6] GOREJOVÁ R., ORIŇAKOVÁ R., ORSÁGOVÁ KRÁLOVÁ Z., SOPČÁK T., ŠIŠOLÁKOVÁ I., SCHNITZER M., KOHAN M., HUDÁK R., *Electrochemical deposition of a hydroxyapatite layer onto the surface of porous additively manufactured Ti6Al4V scaffolds*, Surface and Coatings Technology, 2023, Vol. 455, DOI: 10.1016/j.surfcoat.2022.129207.

[7] JONES D., *Pharmaceutical Applications of Polymers for Drug Delivery*, Rapra Technology Limited, 2004.

[8] KARAMBAKHSH A., AFSHAR A., MALEKINEJAD P., *Corrosion Resistance and Color Properties of Anodized Ti-6Al-4V*, Journal of Materials Engineering and Performance, 2010, Vol. 21, 121–127, DOI: https://doi.org/10.1007/s11665-010-9791-1

[9] KIEL-JAMROZIK M., SZEWCZENKO J., BASIAGA M., NOWIŃSKA K., *Technological capabilities of surface layers formation on implant made of Ti-6Al-4V ELI alloy*, Acta Bioeng. Biomech., 2015, Vol. 17, 31–37, DOI: 10.5277/ABB-00065-2014-03.

[10] KIM S.S., PARK M.S., JEON O., CHOI C.Y, KIM B.S., *Poly(lactide-co-glycolide)/hydroxyapatite composite scaffolds for bone tissue engineering*, Biomaterials, 2006, 27, 1399–1409, DOI: 10.1016/j.biomaterials.2005.08.016.

[11] KUMAR S., SINGH S., QUADIR S.S., JOSHI G., CHOUHAN M., PURI D., CHOUDHARY D., *Polymeric (PLGA-based) nanocomposites for application in drug delivery: Current state of the art and forthcoming perspectives*, Characterization and Fundamental Processing for Pharmaceutical and Medical Device Development, 2024, 277–324, DOI: https://doi.org/10.1016/B978-0-443-18915-9.00004-5

[12] LI J., ZHANG T., LIAO Z., WEI Y., HANG R., HUANG D., *Engineered functional doped hydroxyapatite coating on titanium implants for osseointegration*, Journal of Materials Research and Technology, 2023, Vol. 27, 122–152, DOI: https://doi.org/10.1016/j.jmrt.2023.09.239

[13] LIU X., CHU P.K., DING C., *Surface modification of titanium, titanium alloys, and related materials for biomedical application*, Mater. Sci. Eng. R, 2004, Vol. 47, 49–121, DOI: https://doi.org/10.1016/j.mser.2004.11.001

[14] LUO R., NEU B., VENKATRAMAN S.S., *Surface Functionalization of Nanoparticles to Control Cell Interactions and Drug Release*, Small, 2012, Vol. 8, 2585–2594, DOI: 10.1002/smll.201200398.

[15] MAKADIA H.K., SIEGEL S.J., *Poly Lactic-co-Glycolic Acid (PLGA) as Biodegradable Controlled Drug Delivery Carrier*, Polymers, 2011, Vol. 3, 1377–1397, DOI: https://doi.org/10.3390/polym3031377

[16] MARCINIAK J., *Biomateriały*, Publisher, Gliwice, Poland 2002.

[17] PREZAS P., SOARES M., BORGES J., SILVA J., OLIVEIRA F., GRACA M., *Bioactivity Enhancement of Plasma-Sprayed Hydroxyapatite Coatings through Non-Contact Corona Electrical Charging*, Nanomaterials, 2023, Vol. 13, https://doi.org/10.3390/nano13061058.

[18] SUN T., HUANG J., ZHANG W., ZHENG X., WANG H., LIU J., LENG H., YUAN W., SONG C., *Simvastatin-hydroxyapatite coatings prevent biofilm formation and improve bone formation in implant-associated infections*, Bioactive Materials, 2023, Vol. 21, 44–56, DOI: https://doi.org/10.1016/j.bioactmat.2022.07.028.

[19] SZEWCZENKO J., KAJZER W., GRYGIEL-PRADELOK M., JAWORSKA J., JELONEK K., NOWIŃSKA K., GAWLICZEK M., LIBERA M., MARCINKOWSKI A., KASPERCZYK J., *Corrosion resistance of PLGA-coated biomaterials*, Acta Bioeng. Biomech., 2017, Vol. 19, 173–179, DOI: 10.5277/ABB-00556-2016-04.

[20] SZEWCZENKO J., KAJZER W., KAJZER A., BASIAGA M., KACZMAREK M., ANTONOWICZ M., NOWIŃSKA K., JAWORSKA J., JELONEK K., KASPERCZYK J., *Biodegradable polymer coatings on Ti6Al7Nb alloy*, Acta Bioeng. Biomech., 2019, Vol. 21, 83–92, DOI: 10.37190/ABB-01461-2019-01.

[21] SZEWCZENKO J., *Kształtowanie właściwości fizycznych i chemicznych warstwy wierzchniej implantów ze stopów tytanu dla traumatologii I ortopedii*, Publisher, Gliwice 2014.

[22] VARGA N., HORNOK V., JANOVÁK L., DÉKÁNY I., CSAPÓ E., *The effect of synthesis conditions and tunable hydrophilicity on the drug encapsulation capability of PLA and PLGA nanoparticles*, Colloids and Surfaces B: Biointerfaces, 2019, Vol. 176, 212–218, https://doi.org/10.1016/j.colsurfb.2019.01.012.

[23] WANG M., *Surface Modification of Metallic Biomaterials for Orthopaedic Application*, Materials Science Forum, 2009, 285–290, http://dx.doi.org/10.4028/www.scientific.net/MSF.618-619.285

[24] ZIMA A., *Wpływ dodatków modyfikujących na właściwości hydroksyapatytowych wielofunkcyjnych tworzyw implantacyjnych przeznaczonych na nośniki leków*, PhD dissertation, AGH University, Kraków 2007.